



## Theoretical study of the experimental coordination behavior of *N*-(2-aminophenyl)-*D*-glycero-*D*-gulo-heptonamide to Hg(II) ion

Margarita I. Bernal-Uruchurtu \*, Alejandro J. Metta-Magaña, Jorge A. Guerrero-Álvarez, Reyna Reyes-Martínez, Hugo Tlahuext \*

Centro de Investigaciones Químicas, Universidad Autónoma del Estado de Morelos, Av. Universidad 1001, Cuernavaca 62209, Mexico

### ARTICLE INFO

#### Article history:

Received 2 June 2008

Received in revised form 26 July 2008

Accepted 3 August 2008

Available online 22 August 2008

#### Keywords:

*N*-(2-Aminophenyl)-*D*-glycero-*D*-gulo-heptonamide

2-(*D*-glycero-*D*-gulo-Hexahydroxyhexyl)-benzimidazole

Dehydration

Metal-carbohydrate interactions

Quantum chemistry calculations

### ABSTRACT

The reactivity of *N*-(2-aminophenyl)-*D*-glycero-*D*-gulo-heptonamide (*adgha*), with the group 12 cations, Zn(II), Cd(II), and Hg(II), was studied in DMSO-*d*<sub>6</sub> solution. The studied system showed a selective coordination to Hg(II), and the products formed were characterized by <sup>1</sup>H and <sup>13</sup>C NMR in DMSO-*d*<sub>6</sub> solution and fast atom bombardment (FAB<sup>+</sup>) mass spectra. The expected coordination compounds, [Hg(*adgha*)](NO<sub>3</sub>)<sub>2</sub> and [Hg(*adgha*)<sub>2</sub>](NO<sub>3</sub>)<sub>2</sub>, were observed as unstable intermediates that decompose to bis-[2-(*D*-glycero-*D*-gulo-hexahydroxyhexyl)-benzimidazole-κN]mercury(II) dinitrate, [Hg(*ghbz*)<sub>2</sub>](NO<sub>3</sub>)<sub>2</sub>. The chemical transformation of the complexes was followed by NMR experiments, and the nature of the species formed is sustained by a theoretical study done using DFT methodology. From this study, we propose the structure of the complexes formed in solution, the relative stability of the species formed, and the possible role of the solvent in the observed transformations.

© 2008 Elsevier Ltd. All rights reserved.

## 1. Introduction

The study of chemical interactions between metal ions and bio-molecules is an area of active research because of its fundamental importance for the understanding of many biochemical processes. In particular, metal-carbohydrate interactions are a subject of great interest due to their role in phenomena such as toxic metal metabolism, transport and storage of metals, function and regulation of metallo-enzymes, and the mechanism of action of metal-containing pharmaceuticals.<sup>1–3</sup> Furthermore, the chemistry between carbohydrates and metallic ions in aqueous solution offers the possibility of looking into the coordination ability of the hydroxyl groups of sugars in competition with water molecules.<sup>4,5</sup> Although coordination chemistry plays a central role in these processes, relatively few well-characterized metallic complexes with carbohydrate ligands have been reported.<sup>6</sup> The development of carbohydrate coordination chemistry requires a thorough understanding of the behavior of these compounds as ligands.<sup>7–10</sup> The study of carbohydrates coordination compounds is a challenge, because single crystals suitable for X-ray diffraction measurements are difficult to obtain and conventional NMR spec-

troscopic measurements are not always able to discern the coordination mode.<sup>11</sup> However, carbohydrates properly functionalized with Lewis-basic substituents ('anchoring' groups) may form highly stable complexes with practically all metals, in many cases such complexes behave similarly to those with corresponding carbohydrate-free ligands.<sup>1,12</sup> Amine and amide are frequently used as 'anchoring' groups, where the presence of two potential binding atoms in the last one, oxygen and nitrogen, has shown to be an useful advantage for coordination experiments.<sup>13</sup>

Due to the interest in the coordination behavior of carbohydrates with anchoring groups, we report here the reactivity of *N*-(2-aminophenyl)-*D*-glycero-*D*-gulo-heptonamide (*adgha*), with Zn(II), Cd(II), and Hg(II) ions. The reactions were monitored by <sup>13</sup>C NMR and only for the latter formed a complex. Through various NMR experiments it was possible to observe some interesting features of this reaction. First, the stoichiometry of the complex preparation, 1:1 or 2:1 ligand-metal ratio, led in the early stages of the reaction to different <sup>13</sup>C spectra, suggesting the formation of at least two different complexes: [Hg(*adgha*)]<sup>2+</sup> and [Hg(*adgha*)<sub>2</sub>]<sup>2+</sup>. Second, the compounds formed evolved over time to a single product [Hg(*ghbz*)<sub>2</sub>]<sup>2+</sup>. Aimed at understanding the observed changes in the DMSO solution containing the Hg(II) complexes, mass spectrometry studies and quantum chemistry calculations were done. The purpose of the theoretical part of this study is to rationalize the observed transformations considering two different aspects:

\* Corresponding authors.

E-mail addresses: [mabel@ciq.uaem.mx](mailto:mabel@ciq.uaem.mx) (M. I. Bernal-Uruchurtu), [tlahuext@ciq.uaem.mx](mailto:tlahuext@ciq.uaem.mx) (H. Tlahuext).

(1) the structure of the proposed complexes and their relative stabilities and (2) the discrete interaction of the solvent with the mercury cation. Though the study considers the reaction occurring in the gas phase, the quantum mechanics study will provide a basic framework to interpret the experimental findings in solution.

## 2. Results and discussion

### 2.1. Experimental results

The studied ligand, *N*-(2-aminophenyl)-*D*-glycero-*D*-gulo-heptonamide, which will be referred as *adgha*, is a poly functional molecule. Its crystal structure, in Figure 1, revealed that the N–C–N fragment is planar due to the presence of the aromatic ring, while the hydroxylated chain has a bent conformation. It was also observed that the *adgha* crystal structure is stabilized by intra- and intermolecular H-bonds.<sup>14</sup>

The reaction of *adgha* with  $\text{Hg}(\text{NO}_3)_2 \cdot \text{H}_2\text{O}$  was followed in two different ligand–salt ratios using  $\text{DMSO-}d_6$  as a solvent for each case. When the experiment was done using a 1:1 ratio, the  $^{13}\text{C}$  NMR spectra of the resulting solution showed the presence of [*N*-(2-amino- $\kappa$ *N*-phenyl)-*D*-glycero-*D*-gulo-heptonamide mercury(II)] dinitrate, abbreviated as  $[\text{Hg}(\text{adgha})](\text{NO}_3)_2$ , a single compound. For this complex the chemical shifts were at higher frequencies than the ligand for C1, C3, and C5, with  $\Delta\delta = \delta_{\text{LHg}} - \delta_{\text{L}}$ ; 7.5, 8.5, and 11.3 ppm, respectively, and more moderate for the carbonyl group C7 ( $\Delta\delta = 1.5$  ppm) and to lower frequency for C2 ( $\Delta\delta = -11.0$  ppm). The  $^1\text{H}$  NMR spectra of the solution showed a single signal for the amidic hydrogen atom at 10.12 ppm and broad signals for  $\text{NH}_2$  and OH groups at 8.12 and 4.7 ppm, respectively. Aromatic and aliphatic signals (7.6–7.2; 4.2–3.4 ppm, respectively) have complex patterns. It is remarkable the difference that this group of signals has with the corresponding signals of pure *adgha*, which exhibit quite clean spectra allowing the individual assignment of each hydroxylic proton.<sup>14</sup> The  $^{13}\text{C}$  NMR spectra of the 2:1 experiment solution correspond to a single compound, {bis-[*N*-(2-amino- $\kappa$ *N*-phenyl)-*D*-glycero-*D*-gulo-heptonamide]mercury(II)} dinitrate, hereafter called  $[\text{Hg}(\text{adgha})_2](\text{NO}_3)_2$ . But in this case, the magnitude of the change of chemical shifts compared with the ligand was smaller than for the 1:1 experiment. It was found that C1, C3, and C5 moved to higher frequencies, 4.9, 5.5, and 7.6 ppm, respectively. The carbonyl group, C7, also showed a

weak shift to higher frequency ( $\Delta\delta = 0.9$  ppm), and C2 to lower frequency ( $\Delta\delta = -8.0$  ppm). In both experiments, carbon atoms in the poly hydroxylated chains have similar shift displacements to those observed for *adgha*. In Table 1, we present the complete set of chemical shifts ( $^{13}\text{C}$ , NMR) found for *adgha*,  $[\text{Hg}(\text{adgha})](\text{NO}_3)_2$ , and  $[\text{Hg}(\text{adgha})_2](\text{NO}_3)_2$ .

After 96 h, we found that the  $^{13}\text{C}$  NMR spectra of the solutions resulting from both experiments had changed to an identical new complex. The transformation for the 1:1 ratio experiment was faster than for the 2:1 case. In Figure 2, we present the time evolution of some signals in the spectra of 1:1 experiment. Possible interaction with the counterion is not expected due to the dilution used in these experiments. Furthermore, the use of a high dielectric constant solvent as DMSO ensures a favorable solvation environment for nitrate ion thus preventing its participation in further reactive processes.

At different times for both cases the  $^{13}\text{C}$  spectra showed the appearance of a new signal close to C7 (carbonyl group); the intensity of this new signal grows steadily while the one, corresponding to C7, slowly disappears. Two different sets of signals for each carbon in the poly hydroxylated chain are also found; the set corresponding to the  $[\text{Hg}(\text{adgha})](\text{NO}_3)_2$  complex tends to disappear with time. Similar changes in the  $^1\text{H}$  NMR spectra are also observed. The peak corresponding to the amino group changes in shape and displacement. From the aromatic group centered at 7.3 ppm, the appearance of a new symmetric signal at lower frequencies grows in over time, while the aromatic group disappears almost completely after 120 h. Furthermore, the intensity of the amide proton peak also diminishes as time passes. The chemical shifts of the resulting compound suggest the transformation of  $[\text{Hg}(\text{adgha})](\text{NO}_3)_2$  complex to {bis-[2-(*D*-glycero-*D*-gulo-hexahydroxyhexyl)-benzimidazole- $\kappa$ *N*]mercury(II)} dinitrate, abridged to  $[\text{Hg}(\text{ghbz})_2](\text{NO}_3)_2$ . The suggested transformations, based on the significant chemical shifts changes found for the *ortho*- and *para*-carbon nuclei, are shown in Scheme 1. Due to the donation of the N atom to the metallic ion, these nuclei are deshielded and thus shifted to higher frequencies.

To confirm the dehydration of the ligand upon coordination to Hg(II), an independent synthesis of 2-(*D*-glycero-*D*-gulo-hexahydroxyhexyl)-benzimidazole, (*ghbz*) was done and its  $^{13}\text{C}$  spectra were recorded (data in Table 1). Comparison of the  $^{13}\text{C}$  spectra of the ligand *ghbz* with the  $[\text{Hg}(\text{ghbz})_2](\text{NO}_3)_2$  complex showed that the most affected nuclei in this case is C7, the imidazolic carbon, which is almost 17 ppm shifted to higher frequencies, thus indicating a strong interaction of the benzimidazole moiety with Hg(II). Only three signals appear for the aromatic carbon atoms [130.3 (C1, C2); 123.7 (C3, C6), and 121.2 (C4, C5) ppm], suggesting that the ligand might be involved in at least one dynamic process with

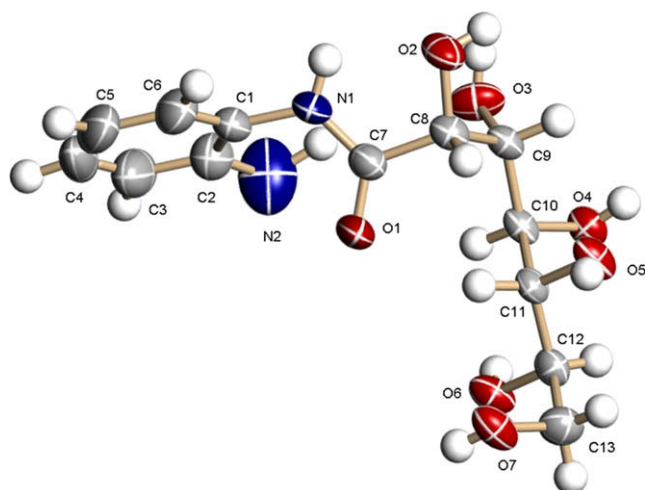


**Figure 1.** Molecular structure of *N*-(2-aminophenyl)-*D*-glycero-*D*-gulo-heptonamide (*adgha*) **1**, showing the atom labeling scheme. Displacement ellipsoids are drawn at the 50% probability level, and H atoms are shown as small spheres of arbitrary radius.

**Table 1**

Summary of  $^{13}\text{C}$  chemical shifts for the species *adgha* (**1**),  $[\text{Hg}(\text{adgha})]^{2+}$  (**2**),  $[\text{Hg}(\text{adgha})_2]^{2+}$  (**3**), *ghbz* (**4**),  $[\text{Hg}(\text{ghbz})_2]^{2+}$  (**5**)  $^1\text{H}$  chemical shifts for N–H and  $\text{NH}_2$  groups;  $\Delta\delta$  (in ppm) are calculated as  $\Delta\delta = \delta_{\text{complex}} - \delta_{\text{ligand}}$  and their corresponding *m/z* found in FAB<sup>+</sup> experiments

	<b>1</b>	<b>2</b>	$\Delta\delta$	<b>3</b>	$\Delta\delta$	<b>4</b>	<b>5<sup>a</sup></b>	$\Delta\delta$
C1	122.8	130.3	7.5	127.7	4.9	138.2	130.3	−7.9
C2	142.5	131.5	−11.0	134.5	−8.0	138.2	130.3	−7.9
C3	115.5	124.0	8.5	121.0	5.5	114.8	123.7	8.9
C4	126.2	127.5	1.3	126.8	0.6	121.4	121.2	−0.2
C5	115.9	127.2	11.3	123.5	7.6	121.4	121.2	−0.2
C6	125.9	127.3	1.4	126.6	0.7	114.8	123.7	8.9
C7	171.9	173.4	1.5	172.8	0.9	156.5	173.4	16.9
N–H ( $\delta$ , $^1\text{H}$ )	9.03	10.12	1.1	10.03	1.0			
$\text{NH}_2$ ( $\delta$ , $^1\text{H}$ )	4.8	8.10	3.3	8.12	3.3			
FAB-MS <i>m/z</i>		833		815		299	797	

<sup>a</sup>  $\delta_{\text{C}}$  68.8 (C8), 78.0 (C9), 67.2 (C10), 71.4 (C11), 67.4 (C12), 62.6 (C13).

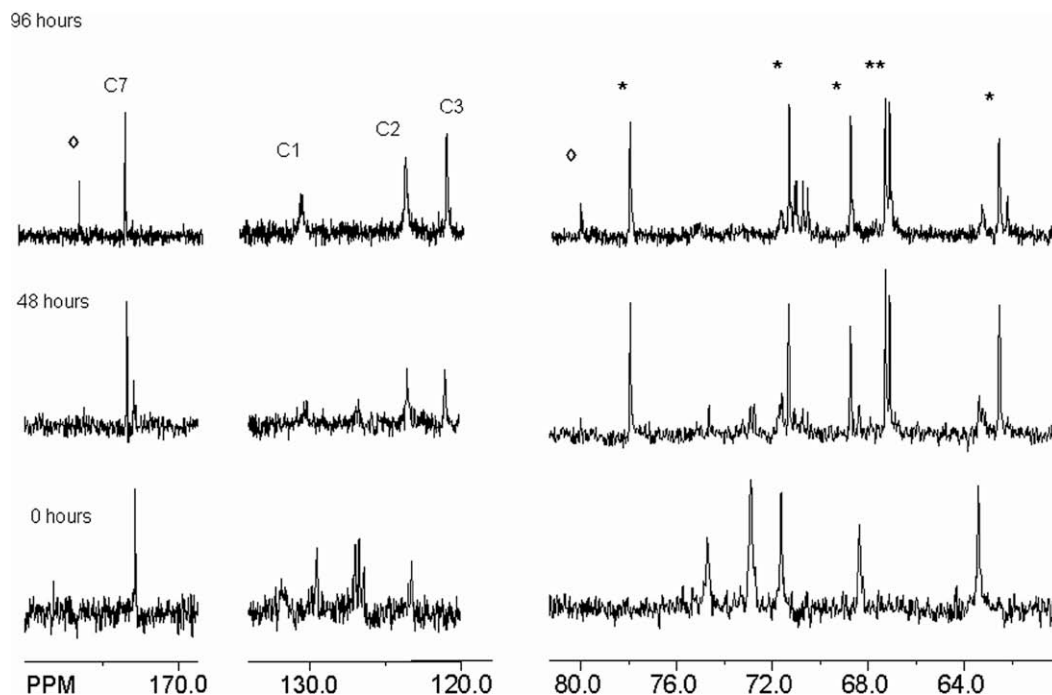
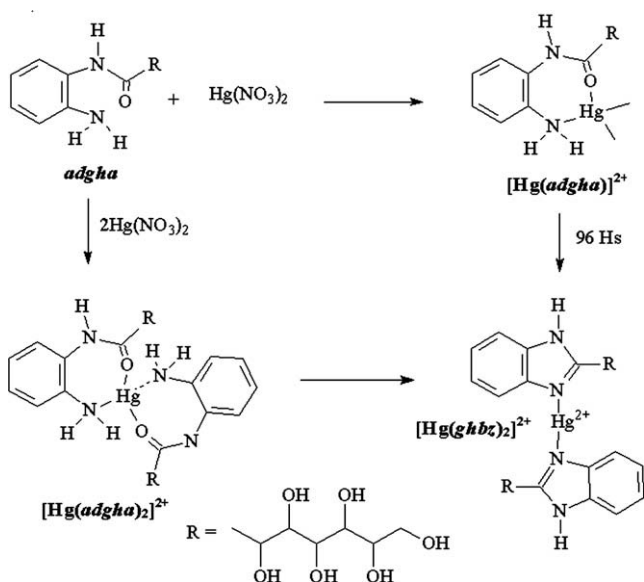


**Figure 2.** Time evolution of the NMR  $^{13}\text{C}$  spectra of the 1:1 reaction between *adgha* and mercury (II) nitrate monohydrate in  $\text{DMSO-}d_6$ . Signals marked with (\*) correspond to carbon nuclei in the hydroxylated chain of the ligand for the  $[\text{Hg}(\text{ghbz})_2]^{2+}$  4, complex and signals marked with (◊) correspond to nuclei in the hydroxylated chain of the hydrolysis product.



**Scheme 1.** Reaction of the *adgha* ligand in two different ligand-salt ratios using  $\text{DMSO-}d_6$  as solvent.

$\text{Hg(II)}$ . It is found that carbon atoms in the poly hydroxylated chain are weakly shifted to lower frequencies than for the free *ghbz*. It is worth mentioning that the preparation of the  $[\text{Hg}(\text{ghbz})_2]^{2+}$  was also attempted starting from *ghbz* and the mercury salt used, but no immediate complex formation was observed. After several days only low intensity peaks of its presence were detected in the  $^{13}\text{C}$  NMR spectra.

The  $\text{FAB}^+$  mass spectra of a fresh sample of the solution from the 1:1 experiment showed the peak corresponding to the molecular ion of the complex  $[\text{Hg}(\text{adgha})_2]^+$   $m/z$  833 ( $M^+$ , 8%), and two other peaks at  $m/z$  815 (35) and  $m/z$  797 (5) suggesting the

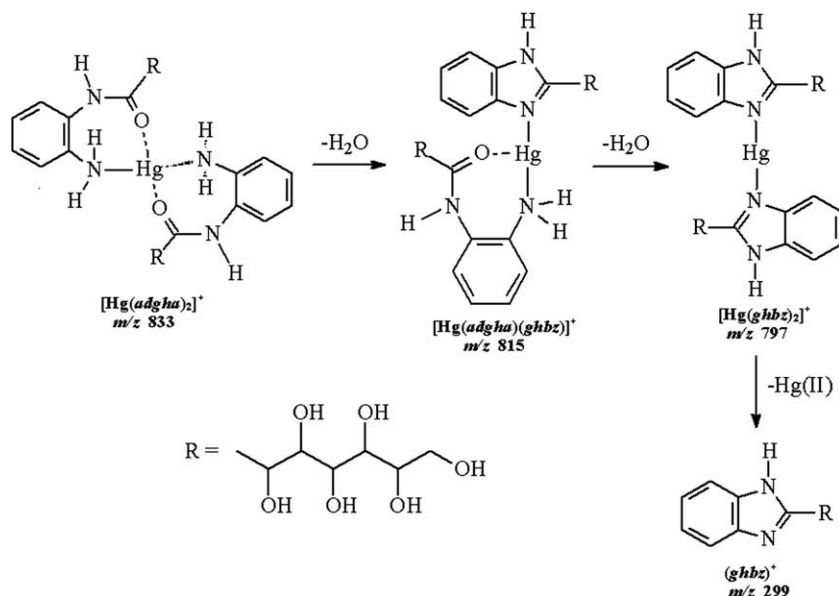
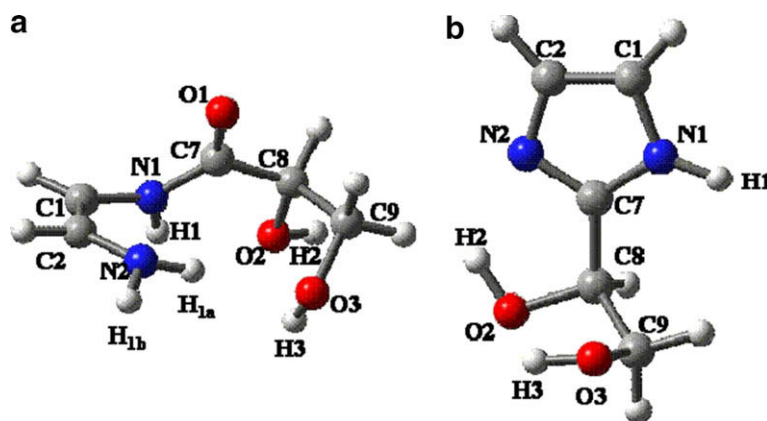
formation of the  $[\text{Hg}(\text{adgha})(\text{ghbz})]^+$  and  $[\text{Hg}(\text{ghbz})_2]^+$  complexes as a result of the loss of one and two water molecules, respectively. Additionally, at  $m/z$  601 (5) appears a peak that corresponds to  $[\text{Hg}(\text{adgha})(\text{DMSO-}d_6)]^+$  and at  $m/z$  516 (7) to  $[\text{Hg}(\text{adgha})]^+$ . It was also possible to observe a very intense peak at  $m/z$  299 (78) that might correspond to the molecular ion of the free *ghbz*. For the 2:1 experiment,  $\text{FAB}^+$  determination found peaks at  $m/z$  833 (7), 815 (12), 797 (5) that, as previously proposed, might correspond to  $[\text{Hg}(\text{adgha})_2]^+$ ,  $[\text{Hg}(\text{adgha})(\text{ghbz})]^+$ , and  $[\text{Hg}(\text{ghbz})_2]^+$ , respectively. In this case, an intense peak at  $m/z$  299 (100) also suggests the presence of the *ghbz*. The general fragmentation pattern is presented in Scheme 2.

It is worth mentioning that for the  $\text{Hg}(\text{NO}_3)_2$  reaction with *adgha*, we found that trace amounts of water in solvent promote the hydrolysis reaction of the amide group followed by amine oxidation and  $\text{Hg}^0$  precipitation. The  $^{13}\text{C}$  NMR spectra allowed for the identification of *D-glycero-D-gulo-heptono-1,4-lactone* as the hydrolysis product.

All our attempts to isolate the expected intermediate complexes  $[\text{Hg}(\text{adgha})(\text{NO}_3)_2]$ ,  $[\text{Hg}(\text{adgha})_2(\text{NO}_3)_2]$ , and  $[\text{Hg}(\text{adgha})(\text{ghbz})](\text{NO}_3)_2$ , as well as the  $[\text{Hg}(\text{ghbz})_2](\text{NO}_3)_2$  complex, were unsuccessful. The quantum mechanics study is aimed to provide a deeper understanding of the coordination behavior of the poly functional ligand *adgha*, the structure around the metal ion, and the geometry of the complexes formed.

## 2.2. Theoretical results

Considering that all NMR spectra coincided in showing that only some atoms of the *adgha* or the *ghbz* ligands were involved in the interaction with  $\text{Hg}^{2+}$ , we decided to model the ligand with only a fragment of it. Our work analyzes the structural and electronic properties of model ligands, in which the glucoheptonic unit was truncated at C9 and the aromatic ring was substituted by a 2-(amino)vinyl group. For convenience, we will maintain the nuclei identification used in Section 4. The model *adgha* and *ghbz*

Scheme 2. FAB<sup>+</sup> fragmentation pattern.

**Figure 3.** Optimized structure for the model ligands (a) model aldonamide ligand *m-adgha*, **1m**; (b) model imidazole ligand *m-ghbz*, **2m**. For convenience, atom labels were maintained from Section 4.

structures were fully optimized at the DFT/B3LYP level, and the optimized structures for both are presented in Figure 3. For the model *adgha* ligand, two stable conformers were found. The first one is 3.6 kcal/mol more stable than the second and is in excellent agreement with the crystal structure of the complete ligand molecule (see Table 2) and for those reasons is the conformer used in this study. The model *adgha* ligand structure is stabilized by two intramolecular H-bonds, one formed between one hydrogen atom of the amino group (H1a) and hydroxylic oxygen (O3) and the other between the hydrogen of the amido group and the O2 hydroxyl group.

The model *adgha* (*m-adgha*) and the resulting model imidazole (*m-ghbz*) were used to study the complex formation with  $\text{Hg}^{2+}$ . For both, we looked at the properties of the 1:1 complexes  $[\text{Hg}(\text{m-adgha})]^{2+}$ ,  $[\text{Hg}(\text{m-ghbz})]^{2+}$ , the bis-ligand complexes (2:1)  $[\text{Hg}(\text{m-adgha})_2]^{2+}$ ,  $[\text{Hg}(\text{m-ghbz})_2]^{2+}$ , and the one containing both ligands  $[\text{Hg}(\text{m-adgha})(\text{m-ghbz})]^{2+}$ . In Figure 4a–e, we present five fully optimized structures, all of them were confirmed as true minima in the corresponding potential energy surface by a frequency analysis. A selection of the most relevant structural parameters (bond

lengths, bond angles, and torsion angles) is presented in Table 2. In addition, we present in Table 3 the complete description of the non-covalent interactions found on these structures. The partial Mulliken charges analysis for ligands and complexes is shown in Table 4.

### 2.2.1. Complexes with the *m-adgha*

The model ligand has five potentially coordinating centers: two hydroxylic oxygen atoms, one carbonyl, one amino group, and one imido nitrogen. Considering the ionic radii of  $\text{Hg}^{2+}$  (1.10 Å) and the conformation of the ligand, the formation of a chelate structure is feasible in at least two different ways. In one, the amino nitrogen N2, the carbonyl oxygen O1, and the hydroxylic O3 bind the cation. In the other, only N2 and O1 participate. Several different initial structures were proposed for the 1:1 complex and after full optimization we found that the most stable structure of  $[\text{Hg}(\text{m-adgha})]^{2+}$  has the carbonyl oxygen O1 and the amino nitrogen N2, as the closest donor atoms to  $\text{Hg}^{2+}$ . We think that this chelate structure is the one formed at the early stages of the reaction and in the 1:1 ratio experiments.

**Table 2**  
Selected experimental structural parameters of *adgha* (**1**) and the corresponding values from the optimized structures of model ligands and complexes, *m-adgha* (**1m**), *m-ghbz* (**2m**),  $[\text{Hg}(m\text{-adgha})_2]^{2+}$  (**3m**),  $[\text{Hg}(m\text{-ghbz})_2]^{2+}$  (**4m**),  $[\text{Hg}(m\text{-adgha})_2]^{2+}$  (**5m**),  $[\text{Hg}(m\text{-ghbz})_2]^{2+}$  (**6m**),  $[\text{Hg}(m\text{-adgha})(m\text{-ghbz})]^{2+}$  (**7m**),  $[\text{Hg}(m\text{-adgha})_2(\text{DMSO})]^{2+}$  (**8m**), and  $[\text{Hg}(m\text{-ghbz})_2(\text{DMSO})]^{2+}$  (**9m**)

	<b>1<sup>a</sup></b>	<b>1m</b>	<b>2m</b>	<b>3m</b>	<b>4m</b>	<b>5m</b>	<b>6m</b>	<b>7m<sup>b</sup></b>	<b>8m</b>	<b>9m</b>
<i>Bond lengths</i> (Å)										
O1–C7	1.221(4)	1.228		1.198		1.247		1.248	1.245	
C7–N1	1.330(5)	1.362	1.363	1.490	1.344	1.350	1.349	1.348	1.350	1.352
N1–C1	1.422(5)	1.424	1.383	1.299	1.383	1.400	1.378	1.408	1.406	1.379
C1–C2	1.388(6)	1.347	1.370	1.462	1.371	1.342	1.365	1.338	1.340	1.365
C2–N2	1.373(8)	1.374	1.379	1.299	1.380	1.435	1.387	1.440	1.431	1.383
C7–N2			1.317		1.345		1.344			1.340
Hg–N2				3.201	2.170	2.258	2.109	2.291, 2.135	2.320	2.148
Hg–O1				3.081		2.422		2.358	2.447	
Hg–O3					2.382		2.524	2.490		2.565
Hg–O <sub>S</sub> <sup>d</sup>									2.349	2.491
<i>Bond angles</i> (°)										
O1–C7–N1	123.5(4)	126.2		118.8		124.7		124.0	124.6	
N2–Hg–O1				56.7		75.9		78.2		
N2–Hg–O3					87.4		82.7		75.7	78.8
O1–Hg–O <sub>S</sub>									102.8	
N2–Hg–O <sub>S</sub>									113.2	
O3–Hg–O <sub>S</sub>										94.1
Hg–O <sub>S</sub> –S									125.5	136.8
N2–Hg–N2 <sup>c</sup>						173.2	168.9	153.5	160.0	170.4
O1–Hg–O1 <sup>c</sup>						116.0			141.7	
O3–Hg–O3 <sup>c</sup>							82.4			80.6
<i>Torsion angles</i> (°)										
C1–N1–C7–O1	0.4(6)	–10.9		–34.4		–15.3		0.7	–11.1	
N2–C2–C1–N1	3.9(7)	2.9	0.2	–32.0	–0.99	–0.4	0.2	–5.2	–1.0	0.0
C7–C8–C9–O3	58.9(4)	63.5	61.8	43.5	60.5	47.7	61.5	54.0, 69.3	53.7	62.6
Hg–O <sub>S</sub> –S–C									125.9, –129.2	–150.5, 106.3

<sup>a</sup> X-ray diffraction data from Ref. 14.

<sup>b</sup> First value corresponds to the *adgha* ligand and second to *ghbz* ligand.

<sup>c</sup> Corresponds to atom in the second ligand unit.

<sup>d</sup> Subscript S corresponds to oxygen atom in DMSO ligand.

The stability of the seven ring structure is reinforced by the presence of the two H-bonds in the ligand structure, one formed between O3 and hydrogen atom of the amino group [N2–H1a···O3] and the other between O2 and the amido hydrogen [N1–H1···O2] (Fig. 4a). Both H-bonds are considerably shorter than in the free ligand, thus suggesting that their presence is of crucial importance for the stability of the chelate ring. An interesting feature of the chelate formed is that, compared to the free ligand structure, the amido-amino system (N1–C1–C2–N2) is no longer planar. A few comments about the electronic modifications that accompany this change are in order. The bond distance pattern in the fragment O1–C7–N1–C1–C2–N2 (1.20, 1.49, 1.30, 1.46, 1.30 Å) differ from those observed in the free ligand (1.22, 1.36, 1.42, 1.35, 1.37 Å), thus suggesting the presence in the complex of a conjugated system with alternating single and double bonds. To fully understand the interaction of this amide with Hg<sup>2+</sup>, we looked in more detail at the nature of the interaction established between the ligand and the metal ion. Thus, a topological analysis of the electronic density in the complex was done using the atoms in molecules theory (AIM). It was possible to locate, besides to the corresponding covalent bonded structure, the critical points corresponding to the coordinative bond between N2, O1, and Hg<sup>2+</sup>. Additionally, a well-defined critical point was located for the two intramolecular hydrogen bonds described above. Interestingly, another critical point was found between O1 and N2, which might have the role of closing the conjugated system upon interaction of the ligand with the metal ion. The charge distribution resulting from conjugation patterns observed for the complex revealed important charge-transfer from the amide ligand to the cation. In particular, it is found that the Hg in the complex has only a +0.24 a.u. charge due to charge transference from the

amide. This density loss is distributed over all the chelate ring members as can be seen from the data in Table 4.

It is not straightforward to advance the structure for the corresponding  $[\text{Hg}(m\text{-adgha})_2]^{2+}$  complex starting from the  $[\text{Hg}(m\text{-adgha})]^{2+}$  properties. First, there was the experimental evidence of the evolution of NMR spectra as function of time, and the observed changes related with the stoichiometry of the experiment. Thus, we decided to perform independent calculations for the  $[\text{Hg}(m\text{-adgha})_2]^{2+}$  system. Two different structures can result depending of the relative orientation of the hydroxylated chains. In one, the hydroxylated chains of both ligands are mutually trans adopting a square planar coordination around Hg<sup>2+</sup>; in the other, these groups are mutually cis. Both starting geometries converged to a single minimum structure, shown in Figure 4c. In this structure the  $[\text{Hg}(m\text{-adgha})_2]^{2+}$  distances are considerably shorter than for the  $[\text{Hg}(m\text{-adgha})]^{2+}$  complex revealing a greater stability. The disposition of the donor atoms around the cation forms a seesaw (SS-4)<sup>15</sup> geometry and in this case the planarity of the N–C=C–N fragment on the ligands is preserved, as well as the single and double bond distances. It is also found that the conformation of the free ligand is, by and large, preserved in the complex, each ligand unit retains two hydrogen bonds (data in Table 3). As a result, the charge transfer to the cation is 0.38 a.u. smaller than for  $[\text{Hg}(m\text{-adgha})_2]^{2+}$ . In contrast to what is found for the  $[\text{Hg}(m\text{-adgha})]^{2+}$  complex, the main charge donors are only the carbonyl oxygen and the amino nitrogen (Table 4).

### 2.2.2. Complexes with *m-ghbz*

The imidazolic ligand has three potential coordination centers. For the  $[\text{Hg}(m\text{-ghbz})_2]^{2+}$  complex all of them participate in the complex formation with Hg<sup>2+</sup> even though this coordination mode

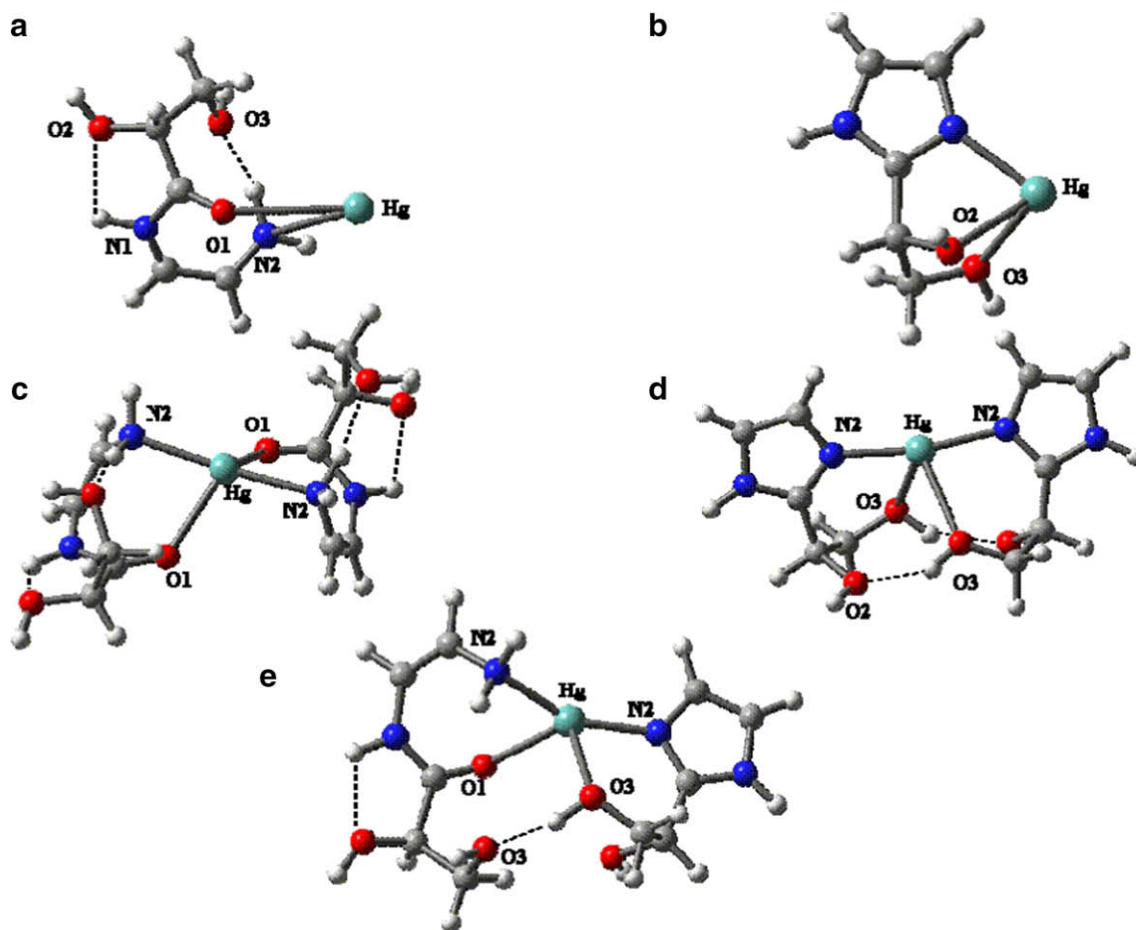


**Figure 4.** Optimized structure of the studied complexes: (a)  $[\text{Hg}(m\text{-adgha})]^{2+}$  (**3m**), (b)  $[\text{Hg}(m\text{-ghbz})]^{2+}$  (**4m**), (c)  $[\text{Hg}(m\text{-adgha})_2]^{2+}$  (**5m**), (d)  $[\text{Hg}(m\text{-ghbz})_2]^{2+}$  (**6m**), (e)  $[\text{Hg}(m\text{-adgha})(m\text{-ghbz})]^{2+}$  (**7m**). Broken lines correspond to the H-bonds mentioned in the text and described in Table 3.

**Table 3**

Hydrogen-bond parameters in *adgha* (**1**), *m-adgha* (**1m**),  $[\text{Hg}(m\text{-adgha})]^{2+}$  (**3m**),  $[\text{Hg}(m\text{-adgha})_2]^{2+}$  (**5m**),  $[\text{Hg}(m\text{-ghbz})_2]^{2+}$  (**6m**),  $[\text{Hg}(m\text{-adgha})(m\text{-ghbz})]^{2+}$  (**7m**),  $[\text{Hg}(m\text{-adgha})_2(\text{DMSO})]^{2+}$  (**8m**), and  $[\text{Hg}(m\text{-ghbz})_2(\text{DMSO})]^{2+}$  (**9m**)

Compound	D–H...A	D–H	H...A	D...A	D–H...A
<b>1<sup>a</sup></b>	N2–H2a–O3	1.05	2.81	3.83	176.3
	N1–H1...O2	0.85	2.13	2.55	110.5
<b>1m</b>	N2–H2a...O3	1.01	2.37	3.38	179.1
	N1–H1...O2	1.01	2.09	2.61	110.4
<b>3m</b>	N2–H2a...O3	1.05	1.74	2.78	167.8
	N1–H1...O2	1.03	2.08	2.49	101.2
<b>5m</b>	N2–H2a...O3	1.04	1.97	3.00	171.1
	N1–H1...O2	1.02	2.00	2.55	110.5
<b>6m</b>	O3–H...O2'	0.98	1.90	2.78	148.4
<b>7m</b>	O3–H...O3'	0.99	1.74	2.70	164.6
	N1–H...O2	1.02	2.05	2.57	109.9
<b>8m</b>	N2–H2a...O3	1.02/1.03	2.64/2.23	3.62/3.23	159.5/162.3
	N1–H1...O2	1.02	2.01/2.04	2.56/2.57	111.0/109.7
<b>9m</b>	O3–H3...O2'	0.98/0.98	1.85/1.82	2.76/2.77	153.0/162.7

Distances are in Å and angles are in degrees.

<sup>a</sup> X-ray diffraction data from Ref. 14.

requires a conformational change of the hydroxylated chain to orientate both hydroxyl groups toward the cation (Fig. 4b). However, this triple coordination to  $\text{Hg}^{2+}$  results in very small charge transference from the ligand to the ion, 0.97 a.u. A different coordination scheme occurs for the  $[\text{Hg}(m\text{-ghbz})]^{2+}$  complex. In this case, the ligands coordinate only through one nitrogen group, N2, and the

oxygen of the final hydroxyl group, O3 (Fig. 4d). The Hg–N distance found for this structure is in good agreement with the bond length values reported for other imidazole mercury complexes, where this bond ranges from 2.20 to 2.29 Å.<sup>16–18</sup> The conformation of the hydroxylic chain favors the formation of two symmetric intramolecular hydrogen bonds between the proton attached to O3 and O2. Those bonds rigidify the structure because they link the two ligand units thus stabilizing the arrangement around  $\text{Hg}^{2+}$ . In this case, we found that the charge transference to  $\text{Hg}^{2+}$  is larger than for  $[\text{Hg}(m\text{-ghbz})]^{2+}$  (1.19 a.u.), but represents a smaller modification for each ligand unit (c.a. 0.60 a.u.).

Because the spectroscopic results showed the transformation of the *adgha* complex to an imidazolic one, we explored the stepwise dehydration of the ligands and the properties of the resulting complexes. First, the transformation of one *adgha* ligand to a *ghbz* in the complex gave the structure shown in Figure 4e. The *adgha* fragment is not significantly modified from the  $[\text{Hg}(m\text{-adgha})]^{2+}$  complex. The imidazole conformation changes to provide, through O3, the fourth donor group to  $\text{Hg}^{2+}$ . In this conformation, the imidazole forms a hydrogen bond (1.74 Å) between the hydrogen on O3 with the hydroxyl group of the *adgha* ligand, that is, there is an intramolecular bond in the complex that links two different ligands around the metallic center. Indeed, the formation of this H-bond is favored over the interaction in *adgha* ligand between the amino group and O3 (3.28 Å). Additionally, it is possible to suggest that a C–H...O interaction (2.54 Å) is formed between both ligands [C9–H...O2'].

**Table 4**  
Mulliken charges for the ligands and the complexes: *m-adgha* (**1m**), *m-ghbz* (**2m**), [Hg *m-adgha*]<sup>2+</sup> (**3m**), [Hg(*m-adgha*)<sub>2</sub>]<sup>2+</sup> (**5m**), [Hg *m-ghbz*]<sup>2+</sup> (**4m**), [Hg(*m-ghbz*)<sub>2</sub>]<sup>2+</sup> (**6m**), [Hg(*m-adgha*)<sub>2</sub>DMSO]<sup>2+</sup> (**8m**), and [Hg(*m-ghbz*)<sub>2</sub>DMSO]<sup>2+</sup> (**9m**)

	1m	2m	DMSO	3m	5m	4m	6m	8m	9m
C7	0.57	0.48	—	0.48	0.51	0.51	0.49	0.52	0.48
C1	0	0.07	—	0.17	0.09	0.08	0.08	0.07	0.07
C2	0.14	0.04	—	0.15	0.05	0.09	0.07	0.06	0.04
N1	−0.55	−0.53	—	−0.37	−0.47	−0.52	−0.48	−0.48	−0.48
N2	−0.61	−0.54	—	−0.43	−0.66	−0.47	−0.56	−0.65	−0.54
O1	−0.51	—	—	−0.29	−0.47	—	—	−0.47	—
O <sub>s</sub>	—	—	−0.63	—	—	—	—	−0.64	−0.66
Hg	—	—	—	0.24	0.62	1.03	0.81	0.53	0.72

Values are expressed in a.u. and atom identification corresponds to labels in Figures 1 and 2.

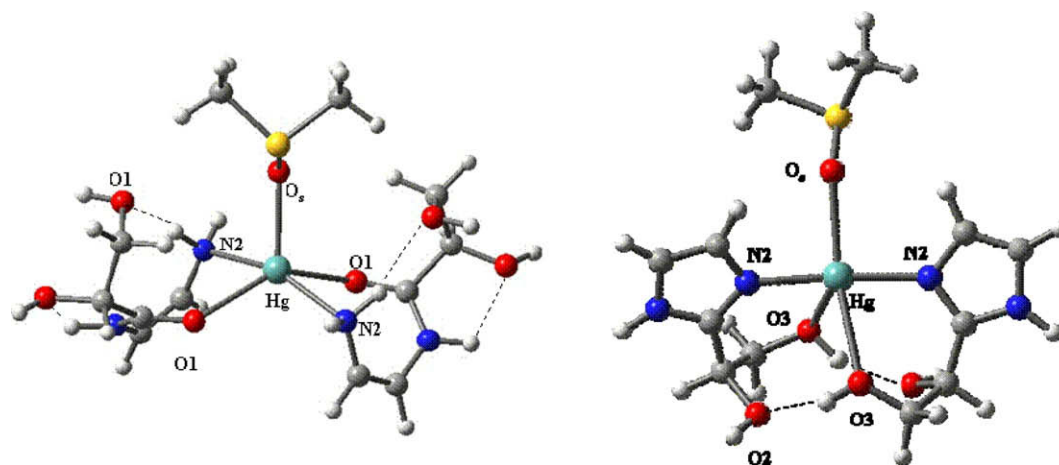


**Figure 5.** Optimized structure of (a) [Hg(*m-adgha*)<sub>2</sub>(DMSO)]<sup>2+</sup> (**8m**) and (b) [Hg(*m-ghbz*)<sub>2</sub>(DMSO)]<sup>2+</sup> (**9m**).

### 2.2.3. Solvent interaction

The solubility of the mercury (II) salt in DMSO indicates that the starting material for the reaction is a solvato-complex of Hg<sup>2+</sup>. Additionally, the structure found for [Hg(*m-adgha*)<sub>2</sub>]<sup>2+</sup>, as well as for [Hg(*m-ghbz*)<sub>2</sub>]<sup>2+</sup>, suggest the possibility of augmenting the coordination number around Hg<sup>2+</sup> with the inclusion of one solvent molecule. In Figure 5a and b, we present the resulting penta-coordinated complexes of [Hg(*m-adgha*)<sub>2</sub>(DMSO)]<sup>2+</sup> and [Hg(*m-ghbz*)<sub>2</sub>(DMSO)]<sup>2+</sup>. The first one has a distorted square planar pyramidal geometry around Hg<sup>2+</sup>, and the second has a trigonal bipyramidal structure. In both cases, coordination with the metallic ion is formed through the oxygen atom in DMSO. We found for the [Hg(*m-adgha*)<sub>2</sub>(DMSO)]<sup>2+</sup> complex a shorter bond than in the [Hg(*m-ghbz*)<sub>2</sub>(DMSO)]<sup>2+</sup> case (2.35 Å vs 2.49 Å). Enlarging the coordination sphere around the Hg<sup>2+</sup> is accompanied by a small lengthening of all the donor atom–Hg distances. The only exception is the [Hg(*m-ghbz*)<sub>2</sub>(DMSO)]<sup>2+</sup> complex in which the O3–Hg<sup>2+</sup> distance change is 0.14 Å, almost three times the change in the other bonds. However, this change leads to a contraction of the H-bond that links both imidazolic units attenuating, to some degree, the energetic cost of this structural modification.

### 2.2.4. The relative stabilities of the Hg-complexes

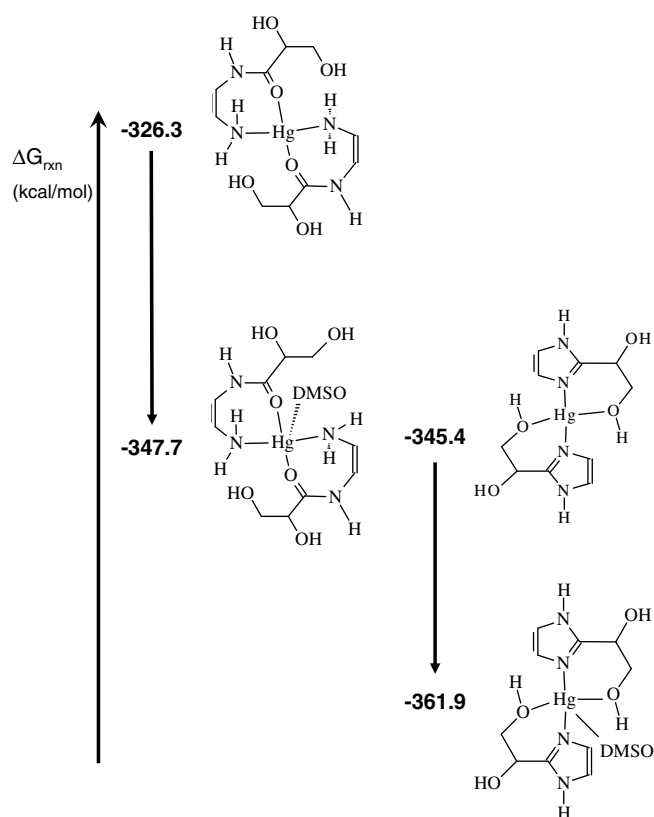
The  $\Delta H$  and  $\Delta G$  for each proposed species was computed using the B3LYP/6-31G(d,p) energies for the optimized structures. These calculations considered the zero-point energy correction and the thermal corrections to the total energy, enthalpy and Gibbs free energy. In Table 5, we present these values, referenced to the energetic values of reactants, Hg<sup>2+</sup> and the corresponding model ligands.

The formation of the 1:1 complexes is 26 kcal/mol more favorable for the [Hg(*m-adgha*)]<sup>2+</sup> than for the [Hg(*m-ghbz*)]<sup>2+</sup> case. The addition of a second unit ligand to the former is quite favorable, with  $\Delta H$  and  $\Delta G$  values of  $-82.3$  kcal/mol and  $-66.9$  kcal/mol, respectively. The ligand dehydration that transforms the [Hg(*m-adgha*)]<sup>2+</sup> to [Hg(*m-ghbz*)]<sup>2+</sup> is also energetically favored and because of the entropic contribution to this reaction. The [Hg(*m-adgha*)(*m-ghbz*)]<sup>2+</sup> complex is close in stability to the [Hg(*m-ghbz*)<sub>2</sub>]<sup>2+</sup> complex. However, because the detection of this species was only possible in the FAB<sup>+</sup> experiments, its presence as an intermediate in the solution reaction is not sustained. From free energy changes, the driving force for the formation of the final single complex appears to be related to the participation of the solvent. The [Hg(*m-ghbz*)<sub>2</sub>(DMSO)]<sup>2+</sup> is  $-14.24$  kcal/mol more stable than [Hg(*m-adgha*)<sub>2</sub>(DMSO)]<sup>2+</sup>, thus spontaneously transforming the expected complex to a different one as shown in Scheme 3.

**Table 5**

Calculated  $\Delta H^\circ$  and  $\Delta G^\circ$  at 298 K and 1 atm for the chemical species proposed for the reaction between *adgha* and Hg(II) in DMSO

		$\Delta H$ (kcal/mol)	$\Delta G$ (kcal/mol)
<b>3m</b>	[Hg( <i>m-adgha</i> )] <sup>2+</sup>	−254.7	−259.4
<b>4m</b>	[Hg( <i>m-ghbz</i> )] <sup>2+</sup>	−228.6	−231.5
<b>5m</b>	[Hg( <i>m-adgha</i> ) <sub>2</sub> ] <sup>2+</sup>	−337.0	−326.3
<b>6m</b>	[Hg( <i>m-ghbz</i> ) <sub>2</sub> ] <sup>2+</sup>	−337.2	−345.4
<b>7m</b>	[Hg( <i>m-adgha</i> )( <i>m-ghbz</i> )] <sup>2+</sup>	−337.3	−336.0
<b>8m</b>	[Hg( <i>m-adgha</i> ) <sub>2</sub> DMSO] <sup>2+</sup>	−368.1	−347.7
<b>9m</b>	[Hg( <i>m-ghbz</i> ) <sub>2</sub> DMSO] <sup>2+</sup>	−364.9	−361.9



Scheme 3. Calculated  $\Delta G_{\text{rxn}}$  for the studied complexes.

### 3. Conclusions

This work looked into the reactivity of an anchored carbohydrate toward ions of groups 12. The anchoring group was selected to provide donor groups of different hardness within the same ligand, and as expected its presence was crucial for the chelation of  $\text{Hg}^{2+}$ .

One of the first striking observations about the reactivity of *N*-(2-aminophenyl)-*D*-glycero-*D*-gulo-heptonamide with group 12 cations is the selectivity observed toward  $\text{Hg}(\text{II})$ . Several factors can be invoked as the components of this behavior. First, the  $\text{Hg}(\text{II})$ -DMSO solvato complex seems to be more labile allowing for an efficient exchange between the solvent molecules and the amide ligand, whereas the equivalent solvato complexes of  $\text{Cd}(\text{II})$  and  $\text{Zn}(\text{II})$  are not labile enough to exchange ligands. Furthermore, the ionic radius of  $\text{Hg}(\text{II})$  allows it to snugly fit in the basin formed by the anchoring group in contrast with  $\text{Cd}(\text{II})$  and  $\text{Zn}(\text{II})$  that find the amino-carbonyl system too large to form a stable chelate. In this respect, we emphasize that the extremely low solubility of the ligand in other solvents impeded additional tests to understand the causes of this apparent selectivity although further calculations might shed some light on this issue.

The observed changes in the early NMR  $^{13}\text{C}$  experiments of the 1:1 reaction strongly suggest the presence of  $[\text{Hg}(\text{adgha})]^{2+}$ , which, after some time, transforms to  $[\text{Hg}(\text{adgha})_2]^{2+}$ . The identity of the donor atoms, the amino nitrogen and the carbonyl group, is well supported by the observed changes on the  $^{13}\text{C}$  spectra and confirmed by the AIM study of  $[\text{Hg}(m\text{-adgha})]^{2+}$ . The smaller  $\Delta\delta$  changes observed in the 2:1 experiment point toward the formation of a bis-complex. In addition, the strong structural and electronic modification found for  $[\text{Hg}(m\text{-adgha})]^{2+}$  coincide well with the observed displacement of  $^{13}\text{C}$  chemical shifts to higher frequencies than for  $[\text{Hg}(m\text{-adgha})_2]^{2+}$ , where the ligand does not change much. It is interesting that despite the non-participation

of hydroxyl groups in the sphere coordination around  $\text{Hg}^{2+}$  its presence perturbs its proton spectra considerably.

For  $\text{Zn}(\text{II})$  and  $\text{Cd}(\text{II})$ , the  $\text{FAB}^+$  experiments showed none of the expected corresponding molecular ions. In contrast, these experiments confirmed the existence of the  $[\text{Hg}(\text{adgha})_2]^+$  and  $[\text{Hg}(\text{ghbz})_2]^+$  species and also suggested the presence of two different types of ligands in the reaction mixture or the rapid transformation of the *adgha* ligand in the *ghbz* one. However, NMR experiments from the early stages of the reaction showed that a single compound was formed. It seems to be a coincidence that the chemical transformation of *adgha* to *ghbz* induced on the mass spectrometer coincides with the phenomena occurring in solution on a different time scale. In this respect, it is important to keep in mind that the ionization processes occurring in the  $\text{FAB}^+$  experiment are not the same as those occurring in solution. This is due to the energetic content of the reactive system, which might induce or accelerate some chemical transformations. However, from our study it is not completely clear how the dehydration process leading to the formation of benzimidazole complexes is triggered.

It is known that  $\text{Hg}^{2+}$  catalyzes the hydrolysis in amides<sup>19</sup> as might well be the case for this system. Moreover, the existence of a critical point closing the chelate ring in  $[\text{Hg}(m\text{-adgha})]^{2+}$  suggests that the formation of this species might be closely related to the hydrolysis of the amide ligand that leads to the imidazole appearance in solution. This hypothesis is also supported by the observation that it takes longer to form the imidazolic complexes starting from  $[\text{Hg}(\text{adgha})_2]^{2+}$ . The role of the solvent cannot be overlooked. The formation of  $[\text{Hg}(m\text{-adgha})_2\text{DMSO}]^{2+}$  might also result in a delay on the apparition of the imidazole species in solution. With respect to the mixed complex  $[\text{Hg}(m\text{-adgha})(m\text{-ghbz})]^{2+}$ , it is important to emphasize that this species is not observed in any solution experiments and it is only a weak signal on the  $\text{FAB}^+$  experiment. This suggests that the energy supplied through the  $\text{FAB}^+$  experiment is a necessary condition for its formation.

### 4. Experimental

#### 4.1. General methods

The *N*-(2-aminophenyl)-*D*-glycero-*D*-gulo-heptonamide was prepared by a previously published procedure.<sup>14</sup> All other chemicals were purchased from commercial sources and used as received. Solution NMR ( $^1\text{H}$ ,  $^{13}\text{C}$ ) spectra were recorded on Varian Gemini 200 spectrometer in  $\text{DMSO}-d_6$ . Chemical shifts are reported in ppm ( $\delta$ ) downfield from internal TMS. The  $\text{FAB}^+$  mass spectra were obtained on a Jeol JMS-700 equipment in a matrix of *m*-nitrobenzylalcohol.

#### 4.2. Reaction of the *N*-(2-aminophenyl)-*D*-glycero-*D*-gulo-heptonamide (*adgha*) with $\text{Cd}(\text{CH}_3\text{CO}_2)_2 \cdot 2\text{H}_2\text{O}$ and $\text{ZnCl}_2$

The treatment of *adgha* (0.060 g, 0.189 mmol) with  $\text{Cd}(\text{CH}_3\text{CO}_2)_2 \cdot 2\text{H}_2\text{O}$  (0.025 g, 0.095 mmol) or  $\text{ZnCl}_2$  (0.013 g, 0.095 mmol) in  $\text{DMSO}-d_6$  (0.5 mL) did not promote any reaction. No significant changes in the chemical shift of  $^{13}\text{C}$  NMR spectra of the solution were observed.

#### 4.3. [*N*-(2-Amino- $\kappa\text{N}$ -phenyl)-*D*-glycero-*D*-gulo-heptonamidemercury(II)] dinitrate $[\text{Hg}(\text{adgha})](\text{NO}_3)_2$

To a solution of *adgha* (0.060 g, 0.189 mmol) in  $\text{DMSO}-d_6$  (0.5 mL) was added  $\text{Hg}(\text{NO}_3)_2 \cdot \text{H}_2\text{O}$  (0.065 g, 0.189 mmol). The reaction mixture was stirred for 10 min at 20 °C. The homogeneous solution was transferred to 5 mm NMR tube.  $\delta_{\text{C}}$  (200 MHz;  $\text{DMSO}-d_6$ ;  $\text{Me}_4\text{Si}$ ), (see Table 1) 73.3 (C8), 75.1 (C9), 68.9 (C10),

73.4 (C11), 72.1 (C12), 63.9 (C13). [(*adgha*)<sub>2</sub>Hg](NO<sub>3</sub>)<sub>2</sub> was found to be an unstable compound (see Section 2).

#### 4.4. Bis-[*N*-(2-amino-κ*N*-phenyl)-*D*-glycero-*D*-gulo-heptonamide] mercury(II) dinitrate [Hg(*adgha*)<sub>2</sub>(NO<sub>3</sub>)<sub>2</sub>]

To a solution of *adgha* (0.060 g, 0.189 mmol) in DMSO-*d*<sub>6</sub> (0.5 mL) was added Hg(NO<sub>3</sub>)<sub>2</sub>·H<sub>2</sub>O (0.032 g, 0.094 mmol). The reaction mixture was stirred for 5 min at 20 °C. The homogeneous solution was transferred to 5 mm NMR tube. δ<sub>C</sub> (200 MHz; DMSO-*d*<sub>6</sub>; Me<sub>4</sub>Si), (see Table 1) 72.8 (C8), 74.7 (C9), 68.3 (C10), 73.0 (C11), 71.6 (C12), 63.4 (C13). [(*adgha*)<sub>2</sub>Hg](NO<sub>3</sub>)<sub>2</sub> was found to be an unstable compound (see Section 2).

#### 4.5. 2-(*D*-glycero-*D*-gulo-Hexahydroxyhexyl)-benzimidazole (*ghbz*)

*D*-glycero-*D*-gulo-Heptono-1,4-lactone (0.5 g, 2.4 mmol) and *o*-phenylenediamine (0.259 g, 2.4 mmol) were suspended in ethanol (10 mL) in a 20 mL reactor. The reactor was closed and heated in an oil bath with a magnetic stirrer at 100 °C for 24 h. Upon cooling of the mixture to room temperature, an amorphous precipitate was formed, which was collected by filtration, washed with ethanol, and air-dried. Yield: 0.140 g, (20%); IR (KBr): ν(O–H) 3452 (br), ν(O–H) 3388 (br), ν(O–H) 3259 (br), ν(N=C) 1621(w), ν(C=C, skeletal vibrations of benzene) 1459 (m) and 1445 (m). Solution <sup>1</sup>H NMR (DMSO-*d*<sub>6</sub>) 7.11–7.16 and 7.48–7.52 (m, 4H, aromatic protons), 3.39–4.00 (m, 7H, aliphatic protons), 5.91, 4.86, 4.62 (br, 7H, imidazolic and hydroxyl protons); δ<sub>C</sub> (200 MHz; DMSO-*d*<sub>6</sub>; Me<sub>4</sub>Si), (see Table 1) 71.6 (C8), 75.6 (C9), 67.3 (C10), 73.6 (C11), 68.1 (C12), 63.3 (C13); MS *m/z* 299 (M<sup>+</sup>, 100%).

#### 4.6. Theoretical methodology

All quantum chemical calculations of this system were done using the GAUSSIAN98 suite of programs.<sup>20</sup> The study was done using DFT methods, which compared to standard ab initio theories require less computational time and storage memory. The B3LYP hybrid functional was chosen because it has been found to conduce to results in fine agreement to those coming from high-level ab initio methods,<sup>21–24</sup> and particularly has proven to have the best performance for bond lengths in coordination compounds of other group 12 cations.<sup>25</sup> All calculations were done using a 6-31G(d,p) basis set for carbon, oxygen, nitrogen, and hydrogen atoms and for mercury an effective core potential function (ECP) was used. We selected the Stuttgart/Dresden ECP<sup>26</sup> since they contain spin-orbit coupling effects that are non-negligible for second and third row transition metals. The topological analysis of the electronic density was made using the theory of atoms in molecules (AIM)<sup>27</sup> with the program EXTREME.<sup>28</sup>

#### Acknowledgments

This work was funded by CONACYT Grants 3562P-E and 38364-E. AJMM thanks for CONACYT scholarship 165770. We would like to express our gratitude to Professors Minhhuu Hô and Alejandro Ramírez for many fruitful discussions.

#### References

- Gyurcsik, B.; Nagy, L. *Coord. Chem. Rev.* **2000**, *203*, 81–148.
- Predki, P. F.; Whitfield, D. M.; Sarkar, B. *Biochem. J.* **1992**, *281*, 835–841.
- Weis, W. I.; Drickamer, K.; Hendrickson, W. A. *Nature* **1992**, *360*, 127–134.
- Escandar, G. M.; Sala, L. F.; González Sierra, M. *Polyhedron* **1994**, *13*, 143–150.
- Gajda, T.; Gyurcsik, B.; Jakusch, T.; Burger, K.; Henry, B.; Delpuech, J.-J. *Inorg. Chim. Acta* **1998**, *275–276*, 130–140.
- Nagy, L.; Szorcik, A. *J. Inorg. Biochem.* **2002**, *89*, 1–12.
- Pellerito, L.; Nagy, L. *Coord. Chem. Rev.* **2001**, *224*, 111–150.
- Junicke, H.; Bruhn, C.; Kluge, R.; Seriani, A. S.; Steinborn, D. *J. Am. Chem. Soc.* **1999**, *121*, 6232–6241.
- Klüfers, P.; Kunte, T. *Angew. Chem., Int. Ed.* **2001**, *40*, 4210–4212.
- Klüfers, P.; Krotz, O.; Ossberger, M. *Eur. J. Inorg. Chem.* **2002**, *6*, 1919–1923.
- Escandar, G. M.; Salas Peregrin, J. M.; González Sierra, M.; Martino, D.; Santero, M.; Frutos, A. A.; García, S. I.; Labadié, G. F. S. L.; Sala, L. F. *Polyhedron* **1996**, *15*, 2251–2261.
- Steinborn, D.; Junicke, H. *Chem. Rev.* **2000**, *100*, 4283–4317.
- Sigel, H.; Martin, R. B. *Chem. Rev.* **1982**, *82*, 385–426.
- Metta-Magaña, A. J.; Reyes-Martínez, R.; Tlahuext, H. *Carbohydr. Res.* **2007**, *342*, 243–253.
- Connelly, N. G.; Damhus, T.; Hartshorn, R. M.; Hutton, A. T. *Nomenclature of Inorganic Chemistry: IUPAC Recommendations 2005*, 1st ed.; RSC Publishing: Cambridge, 2005; pp 175–179.
- Quiroz-Castro, E.; Bernés, S.; Barba-Behrens, N.; Tapia-Benavides, R.; Contreras, R.; Nöth, H. *Polyhedron* **2000**, *19*, 1479–1484.
- Bebout, D. C.; Garland, M. M.; Murphy, G. S.; Bowers, E. V.; Abelt, C. J.; Butcher, R. J. *Dalton Trans.* **2003**, 2578–2584.
- Meihua, H.; Ping, L.; Yun, C.; Jian, W.; Zheng, L. *J. Mol. Struct.* **2006**, *788*, 211–217.
- Makowska-Grzyska, M. M.; Doyle, K.; Allred, R. A.; Arif, A. M.; Debout, D. C.; Berreau, L. M. *Eur. J. Inorg. Chem.* **2005**, *2005*, 822–827.
- Gaussian 98, Revision A.11.3, Frisch, M. J.; Trucks, G. W.; Schlegel, H. B.; Scuseria, G. E.; Robb, M. A.; Cheeseman, J. R.; Zakrzewski, V. G.; Montgomery, Jr., J. A.; Stratmann, R. E.; Burant, J. C.; Dapprich, S.; Millam, J. M.; Daniels, A. D.; Kudin, K. N.; Strain, M. C.; Farkas, O.; Tomasi, J.; Barone, V.; Cossi, M.; Cammi, R.; Mennucci, B.; Pomelli, C.; Adamo, C.; Clifford, S.; Ochterski, J.; Petersson, G. A.; Ayala, P. Y.; Cui, Q.; Morokuma, K.; Rega, N.; Salvador, P.; Dannenberg, J. J.; Malick, D. K.; Rabuck, A. D.; Raghavachari, K.; Foresman, J. B.; Cioslowski, J.; Ortiz, J. V.; Baboul, A. G.; Stefanov, B. B.; Liu, G.; Liashenko, A.; Piskorz, P.; Komaromi, I.; Gomperts, R.; Martin, R. L.; Fox, D. J.; Keith, T.; Al-Laham, M. A.; Peng, C. Y.; Nanayakkara, A.; Challacombe, M.; Gill, P. M. W.; Johnson, B.; Chen, W.; Wong, M. W.; Andres, J. L.; Gonzalez, C.; Head-Gordon, M.; Replogle, E. S.; Pople, J. A.; Gaussian, Inc.: Pittsburgh, PA, 2002.
- Ziegler, T. *Chem. Rev.* **1991**, *91*, 651–667.
- Atanasov, M.; Daul, C. A.; Fowe, E. P. *Monatsh. Chem.* **2005**, *136*, 925–963.
- Shimodaira, Y.; Miura, T.; Kudo, A.; Kobayashi, H. *J. Chem. Theor. Comput.* **2007**, *3*, 789–795.
- Joubert, J.; Delbecq, F. *J. Organomet. Chem.* **2006**, *691*, 1030–1038.
- Amin, E. A.; Truhlar, D. G. *J. Chem. Theor. Comput.* **2008**, *4*, 75–85.
- Andrae, D.; Haeussermann, U.; Dolg, M.; Stoll, H.; Preuss, H. *Theor. Chim. Acta* **1990**, *77*, 123–141.
- Bader, R. F. W. *Atoms in Molecules*; Oxford University Press: New York, 1994.
- Extrem, v.94 rev B; 1994, Biegler-König, F.; Schönbohm, J.; Deraud, R.; Bayles, D.; Bader, R. F. W.